



Contents lists available at ScienceDirect

Journal of Magnetism and Magnetic Materials

journal homepage: www.elsevier.com/locate/jmmm

Research articles

Synthesis and characterization of a family of molecule-based magnets containing methyl-substituted phenyltricyanoethylene acceptors

James A. King Jr., Christopher L. Houser, Ryan E. Corkill, Gordon T. Yee*

Virginia Tech, Department of Chemistry, Blacksburg, VA 24061, United States

1. Introduction

In 1991, Manriquez et al. reported the first room temperature molecule-based magnet, which was synthesized from bis(benzene)vanadium(0) and tetracyanoethylene (TCNE) in dichloromethane [1]. The formula of the magnetic phase is given by $V[TCNE]_x \cdot y(CH_2Cl_2)$ where x is very close to 2 and y is typically small. The reaction is thought to proceed by the production of two TCNE radical anions from one-electron reduction each by the vanadium(0). Each vanadium ultimately is thus oxidized to vanadium(II). Coordinate covalent bonding by each TCNE radical anion via two or more of its nitrogen atom lone pairs to these cations gives rise to a network. However, direct evidence of this structure is limited to EXAFS data [2] because the material is not crystalline.

Since that time, there have been efforts to optimize T_c , the Curie temperature, of this compound by changing to a different source of metal, including hexacarbonylvanadium, $V(CO)_6$ [3]. Researchers have also explored replacing the vanadium with other metals [4–7] and replacing the TCNE with other organic acceptors [8–11] to create new magnetic solids. Relevant to the latter strategy, we have previously examined the replacement of one or two of the CN functional groups on TCNE with phenyl rings to produce phenyltricyanoethylene (PTCE) and dicyanostilbene [12] scaffolds, respectively. An advantage of this approach is that each of the positions on the phenyl ring is a potential site for derivation, thus providing the opportunity to create not just new acceptors, but new families of acceptors in which properties may be systematically varied. The most obvious characteristic that can be manipulated is the reduction potential of the acceptor.

For example, we have reported families of fluoro-substituted PTCEs where up to five fluorine atoms are placed on the phenyl ring [13,14]. Reactions of each of these building blocks with $V(CO)_6$, yield a family of magnetic coordination networks with T_c 's up to 315 K (42 °C) in the case of 2,3,5,6-tetrafluorophenyltricyanoethylene [15]. Higher T_c 's in this family were generally correlated with greater fluorine substitution, hence easier reduction of the acceptor and a lower energy π^* orbital in which the unpaired electron resides. We modeled this behavior qualitatively based on an overlap model used by Carlegrim for $V[TCNE]_2$ [16]. In this model, a better match between the energy of the orbitals

on the metal and organic radical containing unpaired electrons leads to stronger antiferromagnetic direct exchange. Verdagner has made a similar argument for superexchange in Prussian Blue magnets [17]. We noted in our original paper that steric effects due to substitution in the 2- and/or 6-positions (ortho- to the olefin) could also be playing a role and were correlated with higher T_c as well. These effects were ascribed to greater spin density on the nitrogen atoms of the nitrile functional groups that coordinate to the V(II) [13]. For instance, we recently reported the corresponding chloro-substituted PTCEs [18] which largely follow the above trends but because chlorine atoms are larger than fluorine atoms, steric effects appear to play a larger role in determining T_c .

In this contribution, we explore the effects of analogous methyl substitutions on the phenyl ring of PTCE. Because methyl groups are electron donating, making the acceptors more difficult to reduce, the obvious expectation was that T_c of the resulting magnets should always be lower relative to that of the parent PTCE. This was not observed. Reaction of these new acceptors with $V(CO)_6$ results in new ferrimagnets with ordering temperatures that range from 159 K to 244 K. The observed trends in T_c confirm that the localization of spin density due to loss of conjugation is very important and can be enough to overcome the electron donating effects, resulting in unexpectedly higher T_c for certain substitution patterns. These magnetic results are evaluated in the context of trends in electrochemistry and the results of density functional theory (DFT) calculations.

2. Results and discussion

The three mono-methyl-substituted examples (b-d), as well as the 2,6-dimethyl- (e), 2,4,6-trimethyl- (f) and pentamethyl- (g) derivatives were examined and compared to the parent PTCE(a). (Fig. 1) These acceptors were synthesized by modification of a previously reported three-step procedure [19] using commercially available starting materials, appropriately methyl-substituted benzaldehydes. Overall yields from the benzaldehyde ranged from 14 to 30%. Each of these compounds was purified by column chromatography and characterized by 1H NMR, IR, high resolution mass spectrometry and cyclic voltammetry.

* Corresponding author.

E-mail address: gyee@vt.edu (G.T. Yee).<https://doi.org/10.1016/j.jmmm.2019.165953>

Received 8 July 2019; Received in revised form 3 September 2019; Accepted 4 October 2019

Available online 11 October 2019

0304-8853/ © 2019 Elsevier B.V. All rights reserved.

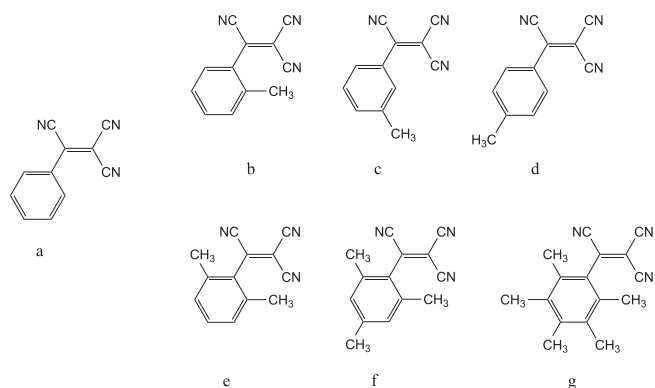


Fig. 1. Methyl-substituted PTCEs investigated herein.

Table 1

Summary of infrared data for six neutral methyl-substituted acceptors and paired with $V(CO)_6$.

| Magnet | Neutral acceptor $\nu_{C=N}$ (cm^{-1}) | Magnetic phase $\nu_{C=N}$ (cm^{-1}) |
|-----------------------|--|--|
| $V(2-MePTCE)_2$ | 2240, 2247 | 2215, 2119 |
| $V(3-MePTCE)_2$ | 2234, 2196 | 2207, 2116 |
| $V(4-MePTCE)_2$ | 2235, 2198 | 2210, 2115 |
| $V(2,6-Me_2PTCE)_2$ | 2240, 2242 | 2202, 2116 |
| $V(2,4,6-Me_3PTCE)_2$ | 2238, 2245 | 2209, 2114 |
| $V(Me_5PTCE)_2$ | 2242, 2264 | 2219, 2113 |

Subsequent reaction of each acceptor with hexacarbonylvanadium (0), in dichloromethane in an inert atmosphere glovebox yields a black insoluble solid that can be isolated by simple vacuum filtration and washing with additional dichloromethane. The resulting materials cannot be dissolved in non-coordinating solvents such as ether or hexanes. The solids were characterized by IR (focusing on the CN stretches) and elemental analysis. The observed CN stretching frequencies for each acceptor are indicative of the oxidation state. (Table 1) Specifically, the absorptions of the neutral acceptor are red-shifted upon one-electron reduction to the radical anion, the form that exists in the magnetic phase. We have previously reported this for PTCE (neutral species; oxidation state = 0) for which the CN stretches are observed 2235 and 2233 cm^{-1} to CN stretches at 2210 and 2129 cm^{-1} for the radical anion (oxidation state = -1) [13].

The elemental analysis for each magnetic phase suggests the stoichiometric ratio of one donor to two acceptors, $V[Me_xPTCE]_2 \cdot yCH_2Cl_2$ (vide infra). This is consistent with all previous reports of similar compounds and results in an overall neutral network of vanadium 2+ cations bridged by radical anions. In each case, the elemental analysis data include approximately 0.5 dichloromethane molecules which are presumed to be solvents of crystallization. Although we have no structural information on these amorphous materials, they are thought to be three-dimensional networks of alternating $S = 3/2$ cations and $S = 1/2$ organic radicals that are antiferromagnetically coupled through direct exchange.

The observed T_c 's of the insoluble networks range from 159 to 244 K. (Table 2) Notably some T_c 's are higher than the parent unsubstituted compound, despite the fact that the methyl group is electron donating, which was predicted to lead to lower T_c . Representative plots of magnetization as a function of temperature (M vs. T) for all six compounds are shown in Fig. 2. T_c values were determined by extrapolating the steep part of the curve to zero and averaging at least two independent measurements. The error in the measurements is ± 3 K. The steepness of each transition suggests that the materials are relatively uniform in composition.

Every new magnet exhibits nearly zero coercivity, consistent with the previously reported TCNE and fluoro- and chloro-substituted

Table 2

Summary of magnetic data for six methyl-substituted acceptors paired with $V(CO)_6$.

| Acceptor | T_c (± 3) K | M_{sat} (emu-G/mol) |
|----------------------------|---------------------|-----------------------|
| PTCE | 215 | 5060 |
| 2-MePTCE | 244 | 4080 |
| 3-MePTCE | 200 | 6260 |
| 4-MePTCE | 182 | 5420 |
| 2,6-Me ₂ PTCE | 241 | 3750 |
| 2,4,6-Me ₃ PTCE | 209 | 5130 |
| Me ₅ PTCE | 159 | 4290 |

compounds and what would be expected for 4A ground state due to vanadium(II) in a presumed pseudo-octahedral ligand field and organic radical anions. A representative example of a plot of M vs. H is shown below for $V[4-MePTCE]_2$. (Fig. 3). The saturation magnetization is roughly the expected value for one net unpaired electron per formula unit (5585 emu-G/mol) and the materials are essentially saturated in a field of 100 G. This is consistent with antiferromagnetic nearest neighbor coupling between two $S = 1/2$ organic radical and the $S = 3/2$ vanadium ion. In a three-dimensional coordination network, this gives rise to bulk ferrimagnetism.

The electronic effects of the methyl group on the properties of each acceptor can be compared to those of the fluoro-group by examining the acid properties of the analogous substituted phenols. The pK_a 's of 2-fluoro-, 3-fluoro- and 4-fluorophenol are 8.81, 9.28 and 9.81 [19], respectively. These values are lower than the pK_a of phenol (9.95), which indicate the fluoro-groups are electron-withdrawing relative to a hydrogen atom. In contrast, the pK_a 's of 2-methyl-, 3-methyl- and 4-methylphenol are 10.28, 10.09 and 10.26, respectively, indicating their weakly electron donating nature [20]. This trend is reflected in reduction potentials of the corresponding methyl-substituted PTCEs as can be seen in Table 3 relative to Ag/AgCl reference electrode, where, as expected, all three monomethyl reductions were more difficult than the parent PTCE and the meta methyl group (3-Me) has the smallest effect. As expected, addition of more methyl groups makes reduction increasingly more difficult.

To address the question of whether there is anything unusual about these data, we have used DFT calculations to determine gas phase electron affinities. The electron affinities were calculated according to protocols recommended by Rienstra-Kiracofe and co-workers [21], where the electron affinity (EA) in our case is the energy of the optimized, neutral acceptor with the energy of the optimized, anionic form of the acceptor subtracted out. Because solvation effects should be similar for all of the acceptors, we expect a linear correlation between these two quantities, as is observed. (Fig. 4).

Plotting electron affinity vs. Curie temperature reveals not a simple linear correlation, but two distinct linear series that are distinguished by the presence or absence of substitution in the 2-position. (Fig. 5) In the former series (blue diamonds), the radical anions are nearly planar in the ground state (vide infra) and the expected electron donating effects of the methyl groups are observed to lower the Curie temperatures. This is based on an overlap model in which the strength of the exchange is correlated with the energy match of the two orbitals that contain unpaired electrons [13].

For the latter series (blue circles), the presence of substitution only ortho- to the olefin (2- or 2,6-), results in magnetic phases with substantially higher T_c 's than that derived from PTCE. This surprising result indicates something other than the simple electron donating effect is operative and suggests that the change in geometry due to steric repulsion can play a large role. From the data, it appears that further addition of methyl groups lowers the T_c , which can be explained by the electron donating effect asserting itself. However, the presence of more methyl groups could also be inhibiting efficient network formation and we cannot rule this out. To gain insight into the contributions to the

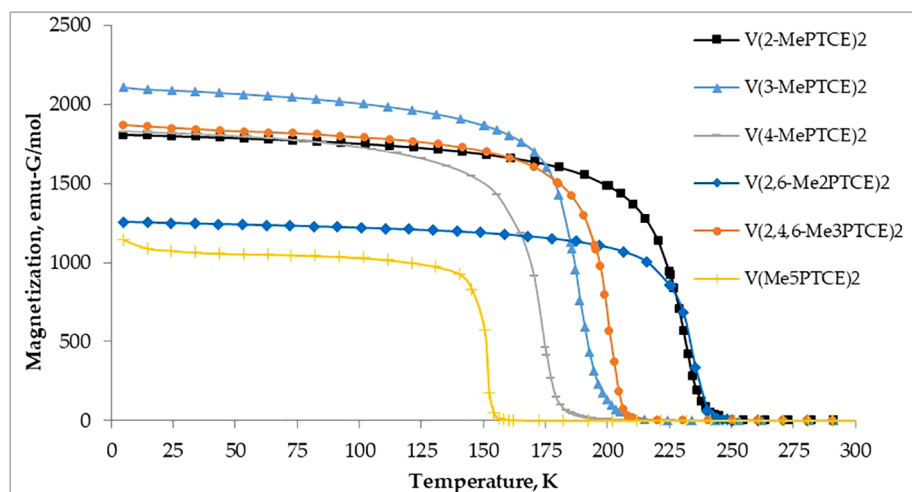


Fig. 2. Magnetization vs. temperature for the six magnets described herein.

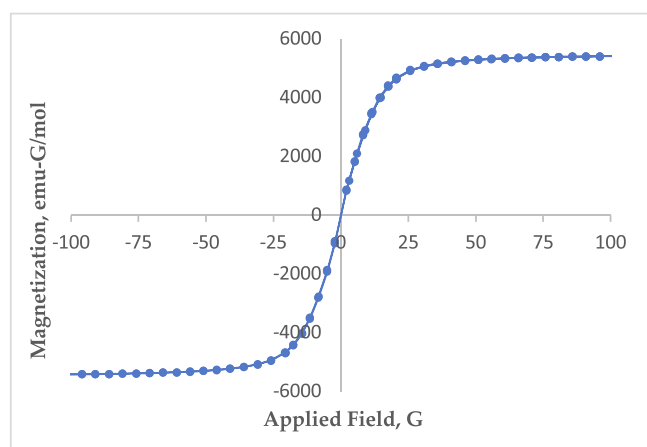


Fig. 3. Magnetization vs. applied field for $V[4\text{-MePTCE}]_2$.

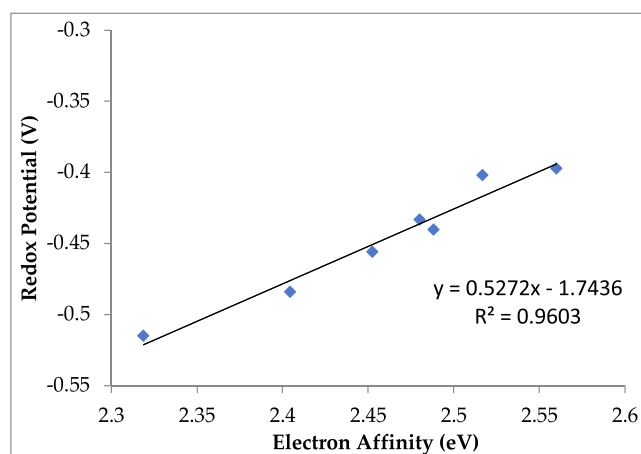


Fig. 4. Linear correlations between experimental redox potential and calculated electron affinity.

Table 3

Electrochemical data for the six acceptors.

| Acceptor | E_{red} (V) | Acceptor | E_{red} (V) |
|----------|----------------------|----------------------------|----------------------|
| PTCE | -0.397 | 2,6-Me ₂ PTCE | -0.456 |
| 2-MePTCE | -0.440 | 2,4,6-Me ₃ PTCE | -0.484 |
| 3-MePTCE | -0.402 | Me ₅ PTCE | -0.515 |
| 4-MePTCE | -0.433 | | |

increased T_c , we used DFT calculations to evaluate the geometry and the spin density distribution of the radical anion.

Within the PTCE molecule or radical anion, one can define a dihedral angle between the plane of the phenyl ring and the plane of the olefin moiety. When the dihedral angle is 0° , the π system of the phenyl ring is fully conjugated with the pi orbitals of the olefin. If the angle is 90° , the two planes of the molecule are orthogonal, and there is no conjugation. DFT calculations indicate that for PTCE, 3-MePTCE and 4-MePTCE radical anions, the ground state is nearly planar at 12° and the barrier to planarity is negligible. Substitution at only the 2-position leads to a minimum in the dihedral angle of about 40° whereas if there is substitution at both the 2- and 6-positions the minimum is at about 65° . (Fig. 6). The barriers to planarity are ~ 0.5 kJ/mol for no substitution in the 2- or 6-positions, ~ 24 kJ/mol for 2-MePTCE and ~ 53 kJ/mol for all acceptors with substitutions in both the 2- and 6-positions.

The loss of conjugation results in localizing greater unpaired spin

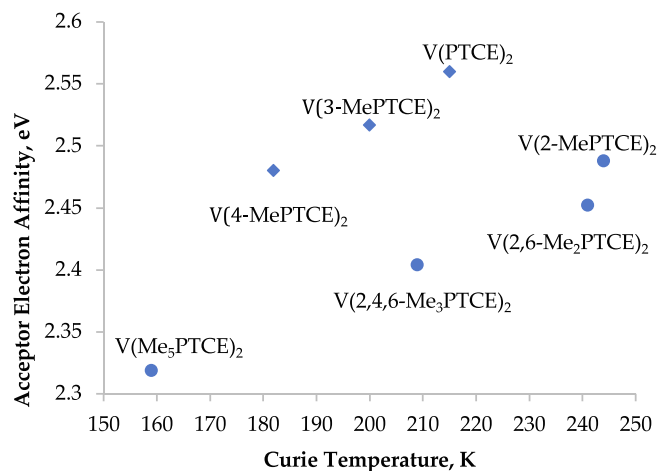


Fig. 5. Electron affinity plotted against Curie temperature.

density on the nitrile nitrogen atoms. Fig. 7 shows that with no substitution in the 2- and/or 6-positions, the total spin density on the nitrogen atoms is largely constant. It increases from 0.42 electrons up to 0.48 electrons as the dihedral angle increases. The added spin density comes at the cost of spin density on the phenyl ring, consistent with the loss of conjugation.

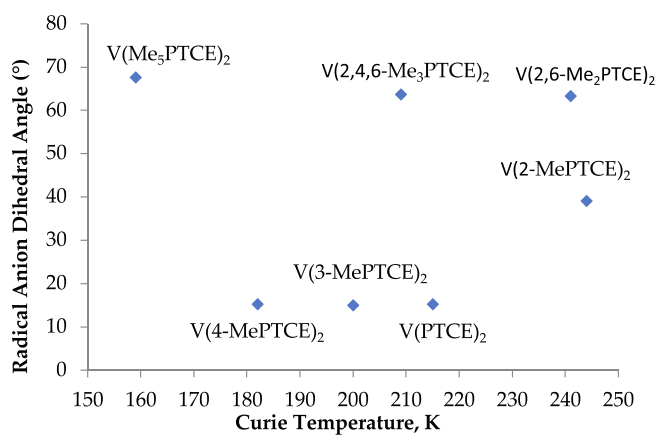


Fig. 6. Dihedral angle plotted against Curie temperature.

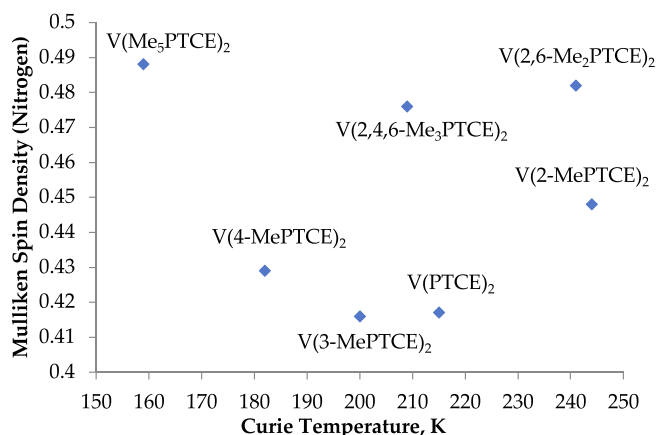


Fig. 7. Total spin density on the nitrile nitrogen atoms plotted against Curie temperature.

Greater spin density on the nitrogen atoms bonded to the vanadium results in greater stabilization of the antiferromagnetically coupled state for Heisenberg Hamiltonian, $H = -2J \sum S_1 \cdot S_2$ [22] where J is the coupling constant and S_1 and S_2 are the spins on the nitrogen atom and vanadium ion, respectively. All other things being equal, larger values of S_1 would yield greater stabilization of the antiferromagnetically coupled state, leading to higher T_c .

Where direct comparisons are possible, all but one of the Curie temperatures of the methyl-substituted PTCE magnets are lower than its fluorine- and chlorine-substituted analogs. (Table 4). The one exception is when substitution is in the 4-(para) position. Although we previously had no good explanation for the extremely low T_c for the magnets derived from 4-FPTCE and 4-ClPTCE, (they are much lower than that for PTCE (213 K), when it was expected to be much higher) we have since identified a possible culprit: a fluorine or chlorine atom on a benzene ring para- to a good electron withdrawing group is susceptible to nucleophilic aromatic substitution [23]. The extremely electron-rich V(0) could react to displace the halogen. Such a reaction would change the

Table 4
Comparison of T_c for methyl-, fluoro-, and chloro-substituted [13,14,18] magnets.

| Substitution position | Methyl | Fluoro | Chloro |
|-----------------------|--------|--------|--------|
| 2- | 244 | 257 | 271 |
| 3- | 200 | 233 | 243 |
| 4- | 182 | 160 | 146 |
| 2,6- | 241 | 300 | 285 |
| Penta- | 159 | 306 | n/a |

identity of the acceptor and/or change the connectivity of the network, providing another pathway for magnetic coupling. Since the methyl group would be a poor leaving group for this reaction pathway, it presumably does not occur, and so a “normal” depression of T_c is observed due to the electron donating ability of the methyl.

To summarize, several molecule-based magnets derived from hexacarbonylvanadium(0) and various methyl-substituted phenyl-tricyanoethylene one-electron acceptors were investigated. Two examples exhibited T_c 's that were surprisingly high based on the expectation of electron-donation as the principal determining factor. For compounds based on essentially planar acceptors that have similar calculated spin densities on the nitrile nitrogen atoms (PTCE, 3-Me and 4-Me) there is a simple correlation between T_c and electron affinity. Substitution at the 2- and/or 6-positions, however, profoundly changes the geometry of the acceptor. DFT calculations suggest a twist to non-coplanarity of the phenyl ring and olefin, placing greater unpaired spin density on the nitrile nitrogen atoms. It is precisely these atoms that are bonded to the vanadium(II) cations and are engaged in direct magnetic exchange. This rationalizes why 2-MePTCE and 2,6-Me₂PTCE support higher T_c 's than the parent PTCE. These results suggest that spin density plays a significant role in the determination of T_c , one at least as important as reduction potential. This, in turn, suggests that the dicyanostilbene family of acceptors, in which two nitrile function groups are replaced with appropriately substituted phenyl rings, pushing even more spin density onto the nitrile nitrogen atoms, could hold some surprises.

3. Experimental

The cyclic voltammetry experiments were performed using a CH Instruments model 600A potentiostat. The measurements were performed on 5 mM solutions in acetonitrile/0.1 M [n-Bu₄N][PF₆] and taken between the potential range of 0 and -700 mV at a scan rate of 100 mV/s using a polished carbon electrode with Ag/AgCl as the reference. Magnetic experiments were performed on a 7 T Quantum Design MPMS SQUID magnetometer. Samples for magnetic experiments were loaded into specially designed tubes in the glovebox, and flame-sealed under vacuum [24]. Experiments involving measurement of magnetization as a function of temperature were performed by first cooling the samples in 50 G and then measuring upon warming from 5 K to 300 K in a 5 G applied field. Measurements involving magnetization as a function of applied field were performed at 5 K. All calculations were performed using the B3LYP density functional with the 6-31+ + G** basis set within Gaussian03 [25]. Beginning with the optimized geometry of PTCE, the neutral and anionic forms of each acceptor were calculated using geometry optimization. From each calculation, the neutral and anionic energies, the Mulliken spin densities and dihedral angles were determined.

The following procedure for the synthesis of the 2-methylphenyl-tricyanoethylene is representative. It is based on a literature procedure [18] and the syntheses for the 3-methyl-, 4-methyl-, 2,6-dimethyl-, 2,4,6-trimethyl-, and pentamethyl acceptors follow the same procedure with minor alterations (noted). All reagents were used as received, except for the following: the dichloromethane used in the magnet synthesis was distilled from P₂O₅, and the V(CO)₆ was prepared, using a procedure from the literature, from [Et₄N][V(CO)₆] [26].

3.1. 2-(2-methylphenyl)-1,1,2-tricyanoethylene, 2-MePTCE

3.1.1. 2-(2-methylphenyl)-1,1-dicyanoethylene (1)

1 equivalent of 2-methylbenzaldehyde (3.573 g, 29.7 mmol) and an excess of malononitrile (2.13 g, 32.2 mmol) were added to ~80 ml of ethanol (100%) in a 100 ml beaker along with a stir bar. The reagents and solvent were stirred until they became uniform, at which time 1 drop of piperidine was added. After stirring for 10 min, the stir bar was removed, and the beaker was covered with parafilm and set aside for

the night. White crystals began to form within two hours of the completion of the reaction. The white crystals were collected the following day, washed with ethanol (95%), and weighed. 2.43 g (49%) of 1 were collected. IR (KBr): $\nu(\text{CN})$, 2232 cm^{-1} and 2177 cm^{-1} . ^1H NMR (400 MHz, CDCl_3) δ 8.06 (m, 1H), 7.46 (m, 2H), 7.31 (m, 2H), 2.41 (s, 3H) ppm versus TMS.

3.1.2. 2-(2-methylphenyl)-1,1,2-tricyanoethane (2)

One equivalent of 1 (1.20 g, 7.13 mmol) was dissolved in 100 ml of ethanol (100%) in a 600 ml beaker with minimal heating. To this solution was added approximately 2 equivalents of KCN (1.04 g, 16.0 mmol) dissolved in ice cold H_2O , along with more ice-cold H_2O in order to fill the beaker to 400 ml. The reaction solution was immediately placed in an ethanol/ H_2O ice bath at $\sim -7^\circ\text{C}$. The reaction was allowed to stir for approximately 1 hr, after which concentrated HCl was added to acidify the solution. Upon adding the HCl, a white solid began to precipitate from the solution. After attaining a pH around 6, the reaction was allowed to stir for 10 min, and the reaction beaker was covered with parafilm containing holes to release gaseous HCN. The beaker was then placed in the refrigerator overnight to allow the product to continue forming. The crystals were collected and washed with cold H_2O the next day and were then dried under vacuum for approximately 4 hr, weighed, and stored. 1.182 g (85%) of 2 were isolated. IR (KBr): $\nu(\text{CN})$, 2249 cm^{-1} and 2261 cm^{-1} . ^1H NMR (400 MHz, CDCl_3) δ 7.59 (m, 2H), 7.37 (m, 1H), 7.27 (m, 1H), 4.69 (d, 1H), 4.18 (d, 1H), 2.41 (s, 3H) ppm versus TMS.

3.1.3. 2-(2-methylphenyl)-1,1,2-tricyanoethylene

One equivalent of 2 (1.10 g, 5.64 mmol) was added to a 250 ml round-bottom flask along with 40 ml of diethyl ether. An excess of *n*-chlorosuccinimide (NCS) was then added with 80 ml of H_2O to the round-bottom, and the 2-layered solution was then stirred until all of the NCS dissolved (~ 30 min). The organic layer turned light yellow in color as more NCS dissolved. After stirring, the aqueous layer was removed using a separatory funnel, and the organic layer was washed 3 times with H_2O and dried with anhydrous Na_2SO_4 . The ether was then removed by rotoevaporation, leaving yellow oil in the bottom of the flask that was dried under vacuum overnight. The resulting solid (yellow, stained with purple) was dissolved in dichloromethane and loaded onto a silica gel flash column with dichloromethane as the mobile phase. The desired product was the first compound to elute off of the column. The product was dried under vacuum, forming a pale-yellow solid that was weighed and stored in the glovebox. Yield: 0.791 g (73%). Mp: 118.2–118.8 $^\circ\text{C}$. IR (KBr): $\nu(\text{CN})$, 2240 cm^{-1} and 2247 cm^{-1} . ^1H NMR (400 MHz, CDCl_3) δ 7.52 (m, 2H), 7.37 (m, 2H), 2.48 (s, 3H) ppm versus TMS. HRMS-ESI (m/z , $[\text{M}-\text{H}]^-$). Calcd for $\text{C}_{12}\text{H}_8\text{N}_3$: 194.2162. Found: 194.0724.

3.2. 2-(3-methylphenyl)-1,1,2-tricyanoethylene, 3-MePTCE

3-MePTCE was synthesized using a similar procedure, using 3-methylbenzaldehyde as the starting material.

3.2.1. 2-(3-methylphenyl)-1,1-dicyanoethylene

Yield: 55%. IR (KBr): $\nu(\text{CN})$, 2230 cm^{-1} and 2195 cm^{-1} . ^1H NMR (400 MHz, CDCl_3) δ 7.71 (s, 1H), 7.68 (m, 2H), 7.41 (m, 2H), 2.40 (s, 3H) ppm versus TMS.

3.2.2. 2-(3-methylphenyl)-1,1,2-tricyanoethane

Yield: 87%. IR (KBr): $\nu(\text{CN})$, 2253 cm^{-1} and 2267 cm^{-1} . ^1H NMR (400 MHz, CDCl_3) δ 7.35 (m, 4H), 4.39 (d, 1H), 4.20 (d, 1H), 2.41 (s, 3H) ppm versus TMS.

3.2.3. 2-(3-methylphenyl)-1,1,2-tricyanoethylene

Yield: 62%. Mp: 109.1–109.8 $^\circ\text{C}$. IR (KBr): $\nu(\text{CN})$, 2234 cm^{-1} and 2196 cm^{-1} . ^1H NMR (400 MHz, CDCl_3) δ 7.79 (m, 2H), 7.45 (m, 2H),

2.44 (s, 3H) ppm versus TMS. HRMS-ESI (m/z , $[\text{M}-\text{H}]^-$). Calcd for $\text{C}_{12}\text{H}_8\text{N}_3$: 194.2162. Found: 194.0724.

3.3. 2-(4-methylphenyl)-1,1,2-tricyanoethylene, 4-MePTCE

4-MePTCE was synthesized using a similar procedure, using 4-methylbenzaldehyde as the starting material.

3.3.1. 2-(4-methylphenyl)-1,1-dicyanoethylene

Yield: 89%. IR (KBr): $\nu(\text{CN})$, 2229 cm^{-1} and 2202 cm^{-1} . ^1H NMR (400 MHz, CDCl_3) δ 7.78 (d, 2H), 7.30 (d, 2H), 2.42 (s, 3H) ppm versus TMS.

3.3.2. 2-(4-methylphenyl)-1,1,2-tricyanoethane

Yield: 88%. IR (KBr): $\nu(\text{CN})$, 2249 cm^{-1} and 2259 cm^{-1} . ^1H NMR (400 MHz, CDCl_3) δ 7.35 (d, 2H), 7.29 (d, 2H), 4.38 (d, 1H), 4.17 (d, 1H), 2.38 (s, 3H) ppm versus TMS.

3.3.3. 2-(4-methylphenyl)-1,1,2-tricyanoethylene

Yield: 28%. Mp: 120.5–121.0 $^\circ\text{C}$. IR (KBr): $\nu(\text{CN})$, 2235 cm^{-1} and 2198 cm^{-1} . ^1H NMR (400 MHz, CDCl_3) δ 7.92 (d, 2H), 7.38 (d, 2H), 2.47 (s, 3H) ppm versus TMS. HRMS-ESI (m/z , $[\text{M}-\text{H}]^-$). Calcd for $\text{C}_{12}\text{H}_8\text{N}_3$: 194.2162. Found: 194.0722.

3.4. 2-(2,6-dimethylphenyl)-1,1,2-tricyanoethylene, 2,6-Me₂PTCE

2,6-Me₂PTCE was synthesized using a similar procedure, using 2,6-dimethylbenzaldehyde as the starting material.

3.4.1. 2-(2,6-dimethylphenyl)-1,1-dicyanoethylene

Yield: 43%. IR (KBr): $\nu(\text{CN})$, 2237 cm^{-1} and 2201 cm^{-1} . ^1H NMR (400 MHz, CDCl_3) δ 8.13 (s, 1H), 7.28 (m, 2H), 7.16 (m, 1H), 2.55 (s, 6H) ppm versus TMS.

3.4.2. 2-(2,6-dimethylphenyl)-1,1,2-tricyanoethane

Yield: 87%. IR (KBr): $\nu(\text{CN})$, 2246 cm^{-1} and 2269 cm^{-1} . ^1H NMR (400 MHz, CDCl_3) δ 7.27 (m, 2H), 7.15 (m, 1H), 4.92 (d, 1H), 4.38 (d, 1H), 2.54 (s, 6H) ppm versus TMS.

3.4.3. 2-(2,6-dimethylphenyl)-1,1,2-tricyanoethylene

Yield: 62%. Mp: 116.8–117.5 $^\circ\text{C}$. IR (KBr): $\nu(\text{CN})$, 2240 cm^{-1} and 2242 cm^{-1} . ^1H NMR (400 MHz, CDCl_3) δ 7.34 (m, 1H), 7.17 (d, 2H), 2.33 (s, 6H) ppm versus TMS. HRMS-ESI (m/z , $[\text{M}-\text{H}]^-$). Calcd for $\text{C}_{13}\text{H}_{10}\text{N}_3$: 208.243. Found: 208.088.

3.5. 2-(2,4,6-trimethylphenyl)-1,1,2-tricyanoethylene, 2,4,6-Me₃PTCE

2,4,6-Me₃PTCE was synthesized using a similar procedure, using 2,4,6-trimethylbenzaldehyde as the starting material.

3.5.1. 2-(2,4,6-trimethylphenyl)-1,1-dicyanoethylene

Yield: 52%. IR (KBr): $\nu(\text{CN})$, 2239 cm^{-1} and 2216 cm^{-1} . ^1H NMR (400 MHz, CDCl_3) δ 8.10 (s, 1H), 6.92 (m, 2H), 2.28 (s, 3H), 2.26 (s, 6H) ppm versus TMS.

3.5.2. 2-(2,4,6-trimethylphenyl)-1,1,2-tricyanoethane

Yield: 85%. IR (KBr): $\nu(\text{CN})$, 2255 cm^{-1} and 2272 cm^{-1} . ^1H NMR (400 MHz, CDCl_3) δ 6.94 (m, 2H), 4.86 (d, 1H), 4.34 (d, 1H), 2.46 (s, 6H), 2.26 (s, 3H) ppm versus TMS.

3.5.3. 2-(2,4,6-trimethylphenyl)-1,1,2-tricyanoethylene

Yield: 33%. Mp: 108.2–108.9 $^\circ\text{C}$. IR (KBr): $\nu(\text{CN})$, 2238 cm^{-1} and 2245 cm^{-1} . ^1H NMR (400 MHz, CDCl_3) δ 6.99 (s, 2H), 2.32 (s, 3H), 2.31 (s, 6H) ppm versus TMS. HRMS-ESI (m/z , $[\text{M}-\text{H}]^-$). Calcd for $\text{C}_{14}\text{H}_{12}\text{N}_3$: 222.270. Found: 222.104.

3.6. 2-(pentamethylphenyl)-1,1,2-tricyanoethylene, Me₅PTCE

Me₅PTCE was synthesized using a similar procedure, using pentamethylbenzaldehyde as the starting material.

3.6.1. 2-(pentamethylphenyl)-1,1-dicyanoethylene

Yield: 63%. IR (KBr): $\nu(\text{CN})$, 2235 cm^{-1} and 2203 cm^{-1} . ¹H NMR (400 MHz, CDCl₃) δ 8.23 (s, 1H), 2.24 (s, 6H), 2.19 (s, 9H) ppm versus TMS.

3.6.2. 2-(pentamethylphenyl)-1,1,2-tricyanoethane

Yield: 78%. IR (KBr): $\nu(\text{CN})$, 2242 cm^{-1} and 2264 cm^{-1} . ¹H NMR (400 MHz, CDCl₃) δ 5.08 (d, 1H), 4.35 (d, 1H), 2.26 (s, 3H), 2.24 (s, 12H) ppm versus TMS.

3.6.3. 2-(pentamethylphenyl)-1,1,2-tricyanoethylene

Yield: 41%. Mp: compound charred at 180 °C. IR (KBr): $\nu(\text{CN})$, 2239 cm^{-1} and 2249 cm^{-1} . ¹H NMR (400 MHz, CDCl₃) δ 2.27 (s, 3H), 2.23 (s, 12H) ppm versus TMS. HRMS-ESI (*m/z*, [M]). Calcd for C₁₆H₁₅N₃: 249.316. Found: 249.127.

All reactions involving the synthesis of the magnets were carried out in a Vacuum Atmospheres Glovebox with N₂ (ultra-high purity) as the atmosphere.

3.7. V[2-MePTCE]₂

Approximately 2.5 equivalents of the acceptor (2-MePTCE, 60.0 mg) were dissolved in roughly 1.0 ml of dichloromethane in a 50 ml round-bottom flask and left to stir (solution was yellow in color). 1 equivalent of V(CO)₆ (25.0 mg) was dissolved in 1.5 ml of dichloromethane in a vial (solution was also yellow in color), and immediately added to the acceptor in solution. The resulting solution turned almost immediately black-green and eventually black. The reaction was allowed to stir for 30 min, after which the precipitate was collected on a medium frit by vacuum filtration. The black solid was washed with dichloromethane until the filtrate ran clear, dried under vacuum for an hour, and then weighed and stored in a vial. Yield: 47.2 mg (89%). IR (KBr): $\nu(\text{CN})$, 2215 cm^{-1} and 2119 cm^{-1} . Anal. Calc. for C₂₄H₁₄N₆V₁·0.32CH₂Cl₂: C, 62.88; H, 3.18; N, 18.09. Found: C, 62.91; H, 3.63; N, 17.70.

All other magnets were synthesized using a procedure similar to the one used to synthesize V[2-MePTCE]₂ and at similar scale.

3.8. V[3-MePTCE]₂

Yield: 90.5%. IR (KBr): $\nu(\text{CN})$, 2207 cm^{-1} and 2116 cm^{-1} . Anal. Calc. for C₂₄H₁₄N₆V₁·0.48CH₂Cl₂: C, 61.50; H, 3.15; N, 17.58. Found: C, 61.55; H, 3.51; N, 17.66.

3.9. V[4-MePTCE]₂

Yield: 80.7%. IR (KBr): $\nu(\text{CN})$, 2210 cm^{-1} and 2115 cm^{-1} . Anal. Calc. for C₂₄H₁₄N₆V₁·0.53CH₂Cl₂: C, 61.08; H, 3.15; N, 17.42. Found: C, 60.97; H, 2.95; N, 18.37.

3.10. V[2,6-Me₂PTCE]₂

Yield: 85.8%. IR (KBr): $\nu(\text{CN})$, 2202 cm^{-1} and 2116 cm^{-1} . Anal. Calc. for C₂₆H₁₈N₆V₁·0.26CH₂Cl₂: C, 64.70; H, 3.83; N, 17.24. Found: C, 64.68; H, 3.67; N, 17.71.

3.11. V[2,4,6-Me₃PTCE]₂

Yield: 79.7%. IR (KBr): $\nu(\text{CN})$, 2209 cm^{-1} and 2214 cm^{-1} . Anal. Calc. for C₂₈H₂₂N₆V₁·0.57CH₂Cl₂: C, 63.33; H, 4.30; N, 15.51. Found: C, 63.32; H, 4.02; N, 16.19.

3.12. V[Me₅PTCE]₂

Yield: 69.6%. IR (KBr): $\nu(\text{CN})$, 2219 cm^{-1} and 2113 cm^{-1} . Anal. Calc. for C₃₂H₃₀N₆V₁·0.35CH₂Cl₂: C, 67.07; H, 5.34; N, 14.51. Found: C, 67.08; H, 5.44; N, 14.49.

Funding

This research was partially funded by the National Science Foundation grant number CHM-0518220.

Acknowledgments

The Authors gratefully acknowledge Mr. Mark Harvey and Drs. Guangbin Wang, Daniel Crawford and Diego Troya for helpful discussions.

Declaration of Competing Interest

The authors declare no conflict of interest. The funders had no role in the design of the study; in the collection, analyses, or interpretation of data; in the writing of the manuscript, and in the decision to publish the results.

References

- [1] J.M. Manriquez, G.T. Yee, R.S. McLean, A.J. Epstein, J.S. Miller, A room temperature molecular/organic-based magnet, *Science* 252 (1991) 1415–1417, <https://doi.org/10.1126/science.252.5011.1415>.
- [2] D. Haskel, Z. Islam, J. Lang, C. Kmetz, G. Srajer, K.I. Pokhodnya, A.J. Epstein, J.S. Miller, Local structural order in the disordered vanadium tetracyanoethylene room-temperature molecule-based magnet, *Phys. Rev. B* 70 (2004) 054422, <https://doi.org/10.1103/PhysRevB.70.054422>.
- [3] J. Zhang, J.S. Miller, C. Vazquez, P. Zhou, W.B. Brinckerhoff, A.J. Epstein, Improved synthesis of the V(tetracyanoethylene)₂(solvent) room temperature magnet: doubling of the magnetization at room temperature, *ACS Symposium Series American Chemical Society, Washington, DC, 1995*, pp. 311–318.
- [4] J. Zhang, J. Ensling, V. Ksenofontov, P. Gütlich, A.J. Epstein, J.S. Miller, [MII(tene)2] · x CH₂Cl₂ (M = Mn, Fe Co, Ni) molecule-based magnets with T_c values above 100 K and coercive fields up to 6500 Oe, *Angew. Chem. Int. Ed.* 37 (1998) 657–660, [https://doi.org/10.1002/\(SICI\)1521-3773\(19980316\)37:5<657::AID-ANIE657>3.0.CO;2-L](https://doi.org/10.1002/(SICI)1521-3773(19980316)37:5<657::AID-ANIE657>3.0.CO;2-L).
- [5] K.I. Pokhodnya, N. Petersen, J.S. Miller, Iron pentacarbonyl as a precursor for molecule-based magnets: formation of Fe[TCNE]₂ (T_c = 100 K) and Fe[TCNQ]₂ (T_c = 35 K), *Inorg. Chem.* 41 (2002) 1996–1997, <https://doi.org/10.1021/ic011288b>.
- [6] K.I. Pokhodnya, E.B. Vickers, M. Bonner, A.J. Epstein, J.S. Miller, Solid solution V_xFe_{1-x}[TCNE]₂·zCH₂Cl₂ room-temperature magnets, *Chem. Mater.* 16 (2004) 3218–3223, <https://doi.org/10.1021/cm049368b>.
- [7] E.B. Vickers, A. Senesi, J.S. Miller, Ni[TCNE]₂ · zCH₂Cl₂ (T_c = 13 K) and V_xNi_{1-x}[TCNE]₂ · zCH₂Cl₂ solid solution room temperature magnets, *Inorg. Chim. Acta* 357 (2004) 3889–3894, <https://doi.org/10.1016/j.ica.2004.04.030>.
- [8] E.B. Vickers, T.D. Selby, J.S. Miller, Magnetically ordered (T_c = 200 K) bis(tetracyanopyrazine)vanadium, V[TCNP]₂·zCH₂Cl₂, *J. Am. Chem. Soc.* 126 (2004) 3716–3717, <https://doi.org/10.1021/ja0397308>.
- [9] E.B. Vickers, I.D. Giles, J.S. Miller, M[TCNQ]₂-based magnets (M = Mn, Fe Co, Ni; TCNQ = 7,7,8,8-tetracyano-p-quinodimethane), *Chem. Mater.* 17 (2005) 1667–1672, <https://doi.org/10.1021/cm047869r>.
- [10] M.L. Taliaferro, M.S. Thorum, J.S. Miller, Room-temperature organic-based magnet (T_c ≈ 50 °C) containing tetracyanobenzene and hexacarbonylvanadate(–I), *Angew. Chem.* 118 (2006) 5452–5457, <https://doi.org/10.1002/ange.200600988>.
- [11] J. Hao, R.A. Davidson, M. Kavand, K.J. van Schooten, C. Boehme, J.S. Miller, Hexacyanobutadiene-based frustrated and weak ferrimagnets: M(HCBB)₂·zCH₂Cl₂ (M = V, Fe), *Inorg. Chem.* 55 (2016) 9393–9399, <https://doi.org/10.1021/acs.inorgchem.6b01565>.
- [12] J.P. Fitzgerald, B.B. Kaul, G.T. Yee, Vanadium [dicyanoperfluorostilbene]₂·yTHF: a molecule-based magnet with T_c ≈ 205 K, *Chem. Commun.* 1 (2000) 49–50, <https://doi.org/10.1039/A907535F>.
- [13] M.D. Harvey, T.D. Crawford, G.T. Yee, Room temperature and near-room temperature molecule-based magnets, *Inorg. Chem.* 47 (2008) 5649–5655, <https://doi.org/10.1021/ic702359g>.
- [14] M.D. Harvey, J.T. Pace, G.T. Yee, A room temperature ferrimagnet, vanadium [pentafluorophenyltricyanoethylene]₂, *Polyhedron* 26 (2007) 2037–2041, <https://doi.org/10.1016/j.poly.2006.09.097>.
- [15] M.K. Amshumali, M.D. Harvey, G.T. Yee, Room temperature and near-room temperature coordination polymer magnets, *Synth. Met.* 188 (2014) 53–56, <https://doi.org/10.1016/j.synthmet.2013.11.023>.
- [16] E. Carleglim, A. Kancierzewska, M.P. de Jong, C. Tengstedt, M. Fahlman, The unoccupied electronic structure of the semi-conducting room temperature molecular

- magnet V(TCNE)₂, Chem. Phys. Lett. 452 (1–3) (2008) 173–177, <https://doi.org/10.1016/j.cplett.2007.12.049>.
- [17] S. Ferlay, T. Mallah, R. Ouahès, P. Veillet, M. Verdaguer, A room-temperature organometallic magnet based on Prussian blue, Nature 378 (1995) 701–703, <https://doi.org/10.1038/378701a>.
- [18] G. Yee, D. Tatum, J. Zadrozny, A new family of high T_c molecule-based magnetic networks: V[x-ClnPTCE]₂•yCH₂Cl₂ (PTCE = Phenyltricyanoethylene), Magnetochemistry 5 (2019) 44–56.
- [19] B.B. Corson, R.W. Stoughton, Reactions of alpha, beta-unsaturated dinitriles, J. Am. Chem. Soc. 50 (10) (1928) 2825–2837, <https://doi.org/10.1021/ja01397a037>.
- [20] P.J. Pearce, R.J.J. Simkins, Acid strengths of some substituted picric acids, Can. J. Chem. 46 (1968) 241–248.
- [21] J.C. Rienstra-Kiracofe, G.S. Tschumper, H.F. Schaefer, S. Nandi, G.B. Ellison, Atomic and molecular electron affinities: photoelectron experiments and theoretical computation, Chem. Rev. 102 (2002) 231–282, <https://doi.org/10.1021/cr990044u>.
- [22] R.L. Carlin, *Magnetochemistry*, Springer-Verlag, Berlin, Germany, 1986 ch. 6. ISBN 0-387-15816-2.
- [23] S.W. Goldstein, A. Bill, J. Dhuguru, O. Ghoneim, Nucleophilic aromatic substitution – addition and identification of an Amine, J. Chem. Educ. 94 (2017) 1388–1390, <https://doi.org/10.1021/acs.jchemed.6b00680>.
- [24] S.P. Sellers, B.J. Korte, J.P. Fitzgerald, W.M. Reiff, G.T. Yee, Canted ferromagnetism and other magnetic phenomena in square planar, neutral, manganese(II) and iron (II) octaethyltetraazaporphyrins, J. Am. Chem. Soc. 120 (1998) 4662–4670, <https://doi.org/10.1021/ja973787a>.
- [25] M.J. Frisch, G.W. Trucks, H.B. Schlegel, G.E. Scuseria, M.A. Robb, J.R. Cheesman, J.A. Montgomery, T. Vreven, K.N.S. Kudin, J.C. Burant, J.M. Millam, S.S. Iyengar, J. Tomasi, V. Barone, B. Mennucci, M. Cossi, G. Scalmani, N. Rega, G.A. Petersson, H. Nakatsuji, M. Hada, M. Ehara, K. Totota, R. Fukuda, J. Hasegawa, M. Ishida, T. Nakajima, Y. Honda, O. Kitao, H. Nakai, M. Klene, X. Li, J.E. Knox, H.P. Hratchian, J.B. Cross, C. Adamo, J. Jaramillo, R. Gomperts, R.E. Stratmann, O. Yazyev, A.J. Austin, R. Cammi, C. Pomelli, J.W. Ochterski, P.Y. Ayala, K. Morokuma, G.A. Voth, P. Salvador, J.J. Dannenberg, V.G. Zakrzewski, S. Dapprich, A.D. Daniel, M.C. Strain, O. Farkas, D.K. Malick, A.D. Rabuck, K. Raghavachari, J.B. Foresman, J.V. Ortiz, Q. Cui, A.G. Baboul, S. Clifford, J. Cioslowski, B.B. Stefanov, G. Lio, A. Liashenko, P. Piskorz, I. Komaromi, R.L. Martin, D.J. Fox, T. Keith, M.A. Al-Laham, C.Y. Peng, A. Nanayakkara, M. Challacombe, P.M.W. Gill, B. Johnson, W. Chen, M.W. Wong, C. Gonzalez, J.A. Pople, Gaussian 03, Revision C.02, Gaussian, Inc., Wallingford CT, 2004.
- [26] X. Liu, J.E. Ellis, Inorg. Synth. 34 (2004) 96–132.